The Journal of Experimental Biology 200, 2987–3002 (1997)
Printed in Great Britain © The Company of Biologists Limited 1997
JEB1280

THE CONTRACTILE PROPERTIES OF THE M. SUPRACORACOIDEUS IN THE PIGEON AND STARLING: A CASE FOR LONG-AXIS ROTATION OF THE HUMERUS

SAMUEL O. POORE*, A. ASHCROFT, A. SÁNCHEZ-HAIMAN AND G. E. GOSLOW JR
Program in Ecology and Evolutionary Biology, Brown University, Providence, RI 02912, USA

Accepted 3 September 1997

Summary

Wing upstroke in birds capable of powered flight is kinematically the most complicated phase of the wingbeat cycle. The M. supracoracoideus (SC), generally considered to be the primary elevator of the wing, is a muscle with a highly derived but stereotyped morphology in modern flying birds. The contractile portion of the SC arises from a ventral sternum, but its tendon of insertion courses *above* the glenohumeral joint to insert on the dorsal surface of the humerus. To clarify the role of the SC during wing upstroke, we studied its contractile and mechanical properties in European starlings (*Sturnus vulgaris*) and pigeons (*Columba livia*), two birds with contrasting flight styles. We made *in situ* measurements of isometric forces of humeral elevation and humeral rotation and, in addition, measured the extent of unrestrained humeral excursion during stimulation of the muscle nerve. We also generated passive and active length–force curves for the SC of each species.

Stimulation of the SC at humeral joint angles of elevation/depression and protraction/retraction coincident with the downstroke–upstroke transition and mid-upstroke produced substantially higher forces of long-axis rotation than elevation. When the humerus was allowed to move (rotate/elevate) during stimulation, we observed rotation about its longitudinal axis of up to 70–80°, but humeral elevations of only 40–60° above the horizontal (as measured in lateral view). In the active length–force experiments, we measured mean (±S.D.) maximal tetanic forces of 6.5±1.2 N for starlings (*N*=4) and 39.4±6.2 N for pigeons (*N*=6), unexpectedly high forces approximately 10 times body weight. The working range of the SC in both species corresponds to the ascending limb (but not the plateau) of the active length–force curve. The potential for greatest active force is high on the ascending limb at joint angles coincident with the downstroke–upstroke transition, a time when the humerus is depressed below the horizontal and rotated forward maximally. As the SC shortens to counterrotate and elevate the humerus during early upstroke, the potential for active force at shorter lengths declines at a relatively rapid rate.

These findings reveal that the primary role of the SC is to impart a high-velocity rotation of the humerus about its longitudinal axis, which rapidly elevates the distal wing. This rapid twisting of the humerus is responsible for positioning the forearm and hand so that their subsequent extension orients the outstretched wing in the parasagittal plane appropriate for the subsequent downstroke. We propose that, at the downstroke–upstroke transition, variable levels of co-contraction of the M. pectoralis and SC interact to provide a level of kinematic control at the shoulder that would not be possible were the two antagonists to work independently.

The lack of a morphologically derived SC in Late Jurassic and Early Cretaceous birds precluded a high-velocity recovery stroke which undoubtedly limited powered flight in these forms. Subsequent evolution of the derived SC capable of imparting a large rotational force to the humerus about its longitudinal axis was an important step in the evolution of the wing upstroke and in the ability to supinate (circumflex) the manus in early upstroke, a movement fundamental to reducing air resistance during the recovery stroke.

Key words: length–force, supracoracoideus muscle, bird flight, flight evolution, flight muscle, flight control, starling, *Sturnus vulgaris*, pigeon, *Columba livia*.

Introduction

The evolution of powered flight in birds from their theropod ancestors, beginning with the Late Jurassic form *Archaeopteryx*, demonstrates a number of advanced musculoskeletal reconfigurations of the shoulder. The recent discoveries of a series of Late Jurassic and Early Cretaceous fossil birds provide insight into this general pattern of reorganization which includes elongation of the coracoids, scapulae aligned with the vertebral column which join the coracoid at an acute angle, a furcula in at least two specimens and, the trait often considered to be critical for powered flight,

*e-mail: Samuel_Poore@Brown.edu

a keeled sternum (for a review, see Chiappe, 1995). The importance of a keeled sternum for the attachment of the M. pectoralis (pars thoracicus), the muscle that powers the downstroke, is readily recognized (but see Pennycuick, 1986). Less appreciated is the importance of the sternal keel for the extensive origin of the M. supracoracoideus (SC) (Olson and Feduccia, 1979). The M. supracoracoideus in modern birds possesses a tendon of insertion that traverses dorsally from its contractile portion *below* the glenoid, through an osseous canal (foramen triosseum), to insert on the dorsal aspect of the proximal humerus. The highly derived morphology of the SC, a characteristic of modern birds capable of powered flight, was not present in *Archaeopteryx* (Ostrom, 1976*a*,*b*; Wellnhofer, 1988, 1993), nor is there firm evidence for its presence in recently described Mesozoic species (Chiappe, 1995; Sanz *et al.* 1996). It is reasonable to assume that the selective advantages must have been high for redirecting the insertion tendon of the SC from its primitive anteroventral insertion on the humerus to the dorsal attachment present in modern birds and that this reconfiguration is functionally important for sustained powered flight (Olson and Feduccia, 1979; Rayner, 1991).

The role most often attributed to the SC is humeral elevation during the upstroke phase of the wingbeat cycle. For many species of birds, the upstroke of the wing, kinematically the most complicated phase of the cycle, involves rapid withdrawal of the wing towards the body to reduce its surface area and inertia. In addition, the wing is rapidly extended at late upstroke into position for the subsequent downstroke (Brown, 1951, 1963; Dial *et al.* 1991; Rüppell, 1975; Simpson, 1983).

To clarify the role of the SC during wing upstroke, we studied its contractile and mechanical properties in European starlings (*Sturnus vulgaris*) and pigeons (*Columba livia*), two birds with contrasting flight styles. We made *in situ* measurements of the isometric forces of humeral elevation and long-axis humeral rotation during stimulation of the SC and, in addition, measured the extent of unrestrained humeral excursion. We also generated passive and active length–force (length–tension) curves for the SC of each species and interpreted these within an evolutionary and functional framework.

Our most significant finding, which was the basis for a preliminary report (Poore *et al.* 1997), reveals that the primary role of the SC is to impart a high-velocity rotation of the humerus about its longitudinal axis. The rapid twisting of the humerus is responsible for positioning the forearm and hand so that the ventral surface of the wing faces laterally at the upstroke–downstroke transition. The muscle's bipinnate architecture, short moment arm across the glenoid and capacity for high force production support this conclusion. The working range of the SC in both species corresponds to the ascending limb of the active length–force curve below the potential for maximum force. In both species, we measured tetanic forces of 7–10 times body weight. The lack of a morphologically derived SC, as indicated by the lack of an acrocoracoid process which directs the tendon of the SC laterally (Ostrom, 1976*a*,*b*), in Late Jurassic and Early Cretaceous birds (e.g. *Archaeopteryx*) precludes a high-velocity recovery stroke which undoubtedly limited powered flight in these forms. Subsequent evolution of the derived SC capable of imparting a large force to the humerus about its longitudinal axis was critical for the evolution of upstroke and, as we propose elsewhere (Ostrom *et al.* 1997), was an important second step in the evolution of an ability to supinate (circumflex) the manus in early upstroke, a movement fundamental to reducing air resistance during recovery.

Materials and methods

We measured the mechanical properties of the M. supracoracoideus (SC) and the wing movements provided by its *in situ* activation in 12 adult pigeons (*Columba livia*) and nine adult European starlings (*Sturnus vulgaris*). We measured the extent of unrestrained humeral rotation and elevation, the isometric forces of humeral long-axis rotation, and active and passive length–force relationships. Birds were administered ketamine (pigeons, $60\,mg\,kg^{-1}$; starlings, $40\,mg\,kg^{-1}$) and xylazine (pigeons, $6\,mg\,kg^{-1}$; starlings, $4\,mg\,kg^{-1}$) intramuscularly to induce deep anesthesia for surgical procedures; supplementary ketamine was given as needed. All birds were captured from wild populations in Rhode Island and Massachusetts and housed in the Brown University Animal Care Facility. The starlings were fed dry dog food and meal worms, and the pigeons were fed cracked corn. Both species were given water (*ad libitum*). This study was performed in accordance with NIH Guidelines on the Use of Animals in Research.

Humeral excursion

We must emphasize for consideration throughout this report that contraction of the SC results in a complicated movement of the humeral head within/across the surfaces of the glenoid. As the SC shortens, the humerus is simultaneously elevated and rotated about its longitudinal axis. The extremes of rotation, resulting in the anterior edge of the deltopectoral crest deflecting below the horizontal during downstroke and a counter-rotation resulting in the anterior edge of the deltopectoral crest deflecting above the horizontal during upstroke, are limited by the coracohumeral and scapulohumeral ligaments, respectively (Sy, 1936; Jenkins, 1993). Between the two extremes, however, the bulbous humeral head possesses extensive freedom of movement which makes its kinematics difficult to describe (Sy, 1936; Simpson, 1983). We restrict our analysis in this report to descriptions of instantaneous windows of humeral elevation and rotation from within this range of complex kinematics. Though limited, these data reveal elements of wing upstroke heretofore not appreciated.

Non-reduced preparations

We measured the extent of humeral elevation and rotation

during direct muscle stimulation *in situ* in intact adult starlings (*N*=3) and pigeons (*N*=3). Following anesthesia, we removed the feathers over the vertebral column and inserted bipolar stimulationg electrodes into the SC percutaneously. Electrodes (pigeons, 100 μm diameter, 1.0 cm exposure; starlings, 50 μm diameter, 0.5 cm exposure) were designed to provide strong intramuscular stimulation but negligible volume-conducted 'cross-talk' to adjacent muscles (M. coracobrachialis posterior and M. pectoralis). In one experiment, volume-conducted electromyograms were assessed from these muscles using silver electrodes (100 μm diameter, 0.5 mm exposure, 0.5 mm intra-tip distance). We hand-held the bird, activated the SC (0.2 ms pulse duration; 60–100 Hz, 2.0 s train duration), and measured the extent of humeral elevation in lateral view [the angle formed by the long axis of the humerus and the dorsal border (vertebral border) of the scapula] and frontal view (the angle formed in the parasagittal plane by the long axis of the humerus and the horizontal) using a protractor. Independent measurements (three trials) were made by two investigators and averaged.

Reduced preparations

We performed acute *in situ* experiments on anesthetized adult starlings (*N*=2) and pigeons (*N*=2) after surgical isolation of the SC. The feathers were removed from the entire left shoulder and the region over the M. pectoralis. We exposed the dorsal musculature by a long mid-line incision through the skin between the scapula and the vertebral column. After bisecting the M. lattisimus dorsi and the M. rhomboideus muscles and cutting the posterior air sacs, we inserted a trachea tube to provide unidirectional ventilation of warmed and humidified air (either a mixture of 60 % N_2, 40 % O_2 or 100 % O_2). Care was taken not to interrupt the muscles' blood supply, and body temperature was maintained at 39 °C with warmed avian Ringer and/or a heat lamp. With exception of the nerve to the SC, all other nerves emerging from the left brachial plexus were severed to prevent their stimulation through reflex activation or volume conduction. Bipolar silver electrodes in contact with the nerve were used for muscle stimulation. We inserted fine wire bipolar electrodes (insulated silver, 100 μm diameter, 0.5 mm tip exposure, 1 mm inter-tip distance) into the SC with the aid of a 25 gauge hypodermic needle to allow recording of electromyographic signals. The M. pectoralis (pars thoracicus) was detached from its insertion on the ventral surface of the deltopectoral crest, and those muscles from the acromion of the scapula and the acrocoracoid process of the coracoid that traverse dorsally over the tendon of insertion tendon of the SC were transected and reflected (M. deltoideus complex and M. propatagialis complex). The bird was mounted onto a heavy frame by clamping the carina of the sternum, the acrocoracoid process of the coracoid and the medial border of the scapula. The protractor was mounted and aligned with the axis of rotation of the humerus. We measured the extent of humeral excursion (elevation and longitudinal rotation) during supramaximal tetanic stimulation of the nerve (0.2 ms pulse duration, 60 Hz, 2–3 s train duration). Independent measurements (three trials) were made by three investigators and the results were averaged. We fixed the humerus to correspond to the instantaneous *in vivo* joint angles of elevation/depression and retraction reported for starlings (Dial *et al.* 1991) (1) at the downstroke–upstroke transition and (2) at mid-upstroke. The same angles were used for pigeons and, in our estimation, are conservative.

Excursions of humeral elevation and rotation

Unrestricted movement

Initially, we allowed the humerus to respond freely to stimulation and muscle shortening. Similar to our procedure with the non-reduced preparations, we made measurements of the extent of humeral elevation using a protractor in lateral view and frontal view. We also examined the extent of humeral rotation by observing the change in orientation of the wing's ventral surface as the SC shortened.

Restricted movement

Subsequently, we inserted a 23 gauge needle into the distal end of the humeral shaft, thereby allowing 'free' rotation but preventing the elevational component of movement. A second, 3.0 cm 26 gauge needle inserted into the distal humeral shaft perpendicular to its longitudinal axis served as a 'dial' against the protractor. Rotational excursion was measured at the two fixed angles of the humerus corresponding to the two kinematic positions. We set the angle of depression, the angle formed by the long axis of the humerus above and below the vertebral column, at −10 ° for the downstroke–upstroke transition and 0 ° for mid-upstroke. The angle of retraction of the humerus, the angle formed by the long axis of the humerus and the long axis of the vertebral column as viewed from above, was 60 ° at the downstroke–upstroke transition and 30 ° at the mid-upstroke.

Isometric forces of humeral elevation and rotation (torque)

We measured *in situ* isometric elevational force and rotational force applied to the humerus by the SC in each species. A short piece of silk (compliance 0.45 $\mu m N^{-1} cm^{-1}$), tied around the mid-shaft of the humerus at one end and attached to the force transducer at the other, transmitted the force of elevation but allowed for rotation during nerve stimulation (0.2 ms pulse duration, 60 Hz, 500 ms train duration). We estimated the force of elevation at the wing's center of mass at the two wing positions by proportionality using the known force and lever arm lengths. The wing's center of mass was determined by freezing the left wing at the appropriate elbow and wrist joint angles and placing the wing on a pivot (1.5 mm diameter) oriented perpendicular to the ventral surface of the wing. We moved the pivot until a horizontal balance was reached; this position was taken to be the center of mass.

For the isometric rotational force measurements, we drilled a small hole in the deltopectoral crest (with a drimmel tool) through which we threaded a short piece of silver wire (0.38 mm diameter). We attached the wire to the force

transducer mounted below the wing. The distal end of the humerus was stabilized as described above by inserting a 23 gauge needle into its shaft.

Length–force relationships

We derived active and passive length–force curves for the SC by direct nerve stimulation following isolation of the tendon of insertion in adult starlings (N=4) and pigeons (N=8). The tendon of the SC was prepared by retracting the deltoid and propatagialis muscles from the dorsal aspect of the humerus, cutting the bone around the tendon's site of attachment using a drimmel tool, and removing the bone chip along with the tendon. This tendon/bone structure served as a sturdy attachment for the force transducer. Before we removed the tendon and bone chip, a marker was placed on the scapula for later correlation of tendon length to humeral joint angles *in vivo*. We fastened the bone/tendon structure to the force transducer with a 5-0 gauge silk tie after the bird had been stabilized by clamping the sternal keel, proximal coracoid and vertebral margin of the scapula to a heavy frame. The force transducer was mounted on an adjustable rack and pinion (millimeter calibration) above the tendon of the SC, which allowed incremental muscle length change.

We measured the muscle's passive and active length–force properties at a series of lengths encompassing the muscle's normal *in vivo* excursion. The active length–force curves were generated from maximal twitch responses (supramaximal stimulus, 0.2 ms pulse duration) so as not to damage or fatigue the muscle by repeated tetanus. Each curve was generated by lengthening the muscle in 1.0 mm increments over its physiological working range. Between each measurement, we returned the muscle to the length for 'zero' passive tension, waited 5.0 s, and then pulled the muscle to a new longer length. We waited 2.0 s before either measuring the passive force or stimulating the nerve (active series). At the end of each experiment, we measured maximum whole-muscle tetanic force (0.2 ms pulse duration, 60 Hz, 500 ms train duration) at the length coincident with maximum twitch force. We measured the muscle's twitch contraction time (time-to-peak force) from the onset of the electromyogram to peak force at the same length. All data were digitally recorded (10 MHz) and stored on disk for off-line analysis on a Nicolet 400 series waveform acquisition system.

We correlated absolute muscle length to humeral angle of elevation and depression by manipulating the contralateral wing in each bird after it had been killed (sodium pentobarbital, 100 mg kg^{-1}). We dissected the origin of the SC from its membranous and skeletal attachments, mounted the bird in a stereotaxic frame and attached the free belly of the SC to an adjustable rack and pinion. This configuration allowed us to manipulate wing elevation, depression and rotation, and to correlate these with changes in tendon excursion. We manipulated the humerus throughout the *in vivo* excursion range in 10 ° increments above and below the horizontal, which allowed us to correlate the twitch force at each muscle length to its corresponding wing angle.

Results

Myology

The general arrangement of the M. supracoracoideus in birds is given by George and Berger (1966). We employ the nomenclature set forth in *Nomina Anatomica Avium* (Baumel, 1979). In the starling and pigeon, the M. supracoracoideus lies deep to the M. pectoralis pars thoracicus (primarily the sternobrachialis) in both species (Fig. 1). Its fascicles arise from the dorsal half of the carina, from the adjacent body of the sternum, from a small area on the base of the coracoclavicular membrane and from the coracoid adjacent to the coracosternal joint. The tendon of insertion passes dorsally through the triosseal canal (formed by the coracoid, scapula and furcula) and courses anterolaterally to insert on the dorsal surface of the proximal humerus, on the external tuberosity (tuberculum dorsale) above the glenohumeral joint (Figs 1, 2). The bipinnate architecture of the SC is evident in both species. The anterodorsal- and posterodorsal-oriented fascicles attach to a central tendonous sheath (membrane) in the muscle's belly which courses dorsally as the tendon of insertion. The anterodorsally oriented fascicles, those arising from the carina and the sternum, are longer than the posterodorsal fascicles which arise from the coracoclavicular membrane. In the starling, a small sesamoid bone, the Os humerocapsularis, is embedded in M. deltoideus cranialis and attaches to the SC

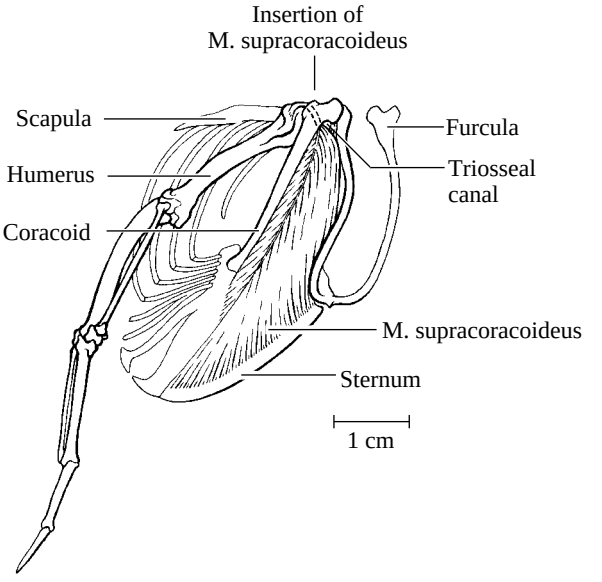

Fig. 1. Anterolateral view of the right shoulder of a European starling (*Sturnus vulgaris*). The pectoralis has been removed as well as all other wing and shoulder musculature to expose the M. supracoracoideus (SC) and its tendon of insertion on the dorsal aspect of the humerus, a position *above* the glenohumeral joint. The fascicles of the SC arise from the dorsal half of the carina of the sternum, the adjacent body of the sternum and a small area on the base of the sterno-coraco-clavicular membrane (see Fig. 2). Note the bipinnate architecture of the SC with its relatively short and oblique fascicles. This fascicle architecture limits shortening excursion but maximizes force production.

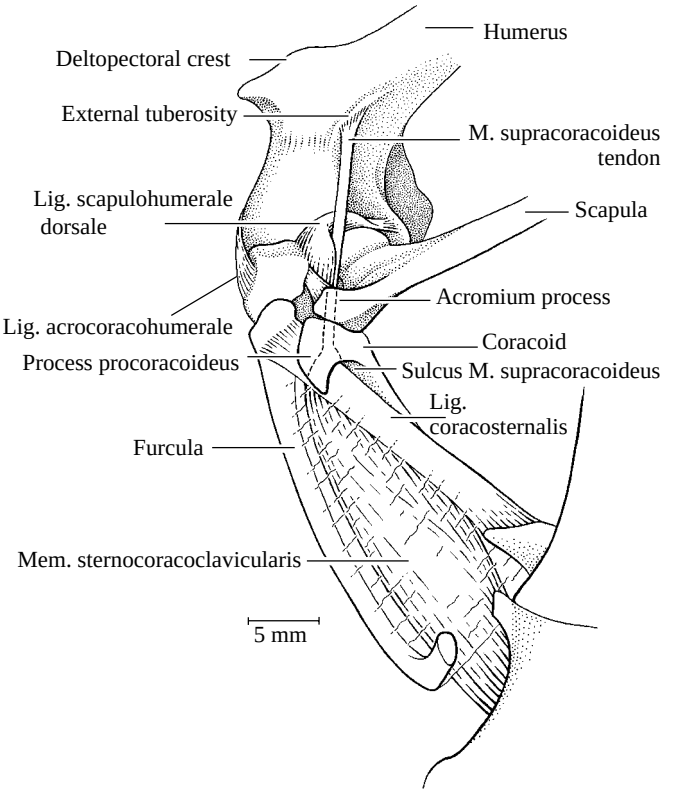

Fig. 2. Dorsomedial view of the right shoulder of an adult pigeon (*Columba livia*). All musculature other than the M. supracoracoideus (SC) has been removed. The belly of the SC is obscured in part by the thin sterno-coraco-clavicular membrane anteriorly and a heavy coracosternal ligament posteriorly. The muscle's free tendon passes lateral to the procoracoid process of the coracoid within the sulcus M. supracoracoideus, through the triosseal canal (see Fig. 1) and inserts onto the external tuberosity (tuberculum dorsale) of the dorsal aspect of the humerus.

tendon by a small tie ligament. This ligament redirects the tendon of the SC anteriolaterally (see Fig. 5; Fig. 3 in Dial *et al.* 1991).

Elevation and rotation of the humerus

The SC of both species elevates and simultaneously rotates the humerus about its long axis, an extremely complex movement. The two movements are presented separately for the purposes of description, but their interrelationship should be kept in mind. The cinematographic records of Jenkins *et al.* (1988) of the wingbeat cycle of a European starling flying in a wind tunnel serve to provide orientation to the general kinematics of wing upstroke (Fig. 3). The key humeral movements during upstroke include retraction–protraction (expressed in terms of the angle between the long axis of the bone and the longitudinal axis of the body), rotation about its longitudinal axis and elevation (the angle between the vertebral border of the scapula and the long axis of the bone as seen in lateral view). The downstroke–upstroke transition is characterized by initiation of retraction, elevation and rotation of the humerus, flexion of the elbow and flexion/supination of the carpometacarpus (wrist) (Fig. 3A). By mid-upstroke, the humerus is maximally retracted and the elbow and wrist are maximally flexed (Fig. 3B). Late upstroke (Fig. 3C) is characterized by protraction/elevation of the humerus and extension of the elbow and wrist. Humeral elevation, as seen in lateral view, is typically 40–60 ° above the horizontal.

These cinematographic records, coupled with our observations during *in situ* stimulations, provide details of how the simultaneous retraction/protraction, rotation and elevation of the humerus during upstroke contribute to the appropriate repositioning of the wing for the subsequent downstroke (Figs 4, 5). At the downstroke–upstroke transition, the humerus may be depressed by 10–20 ° below the horizontal as

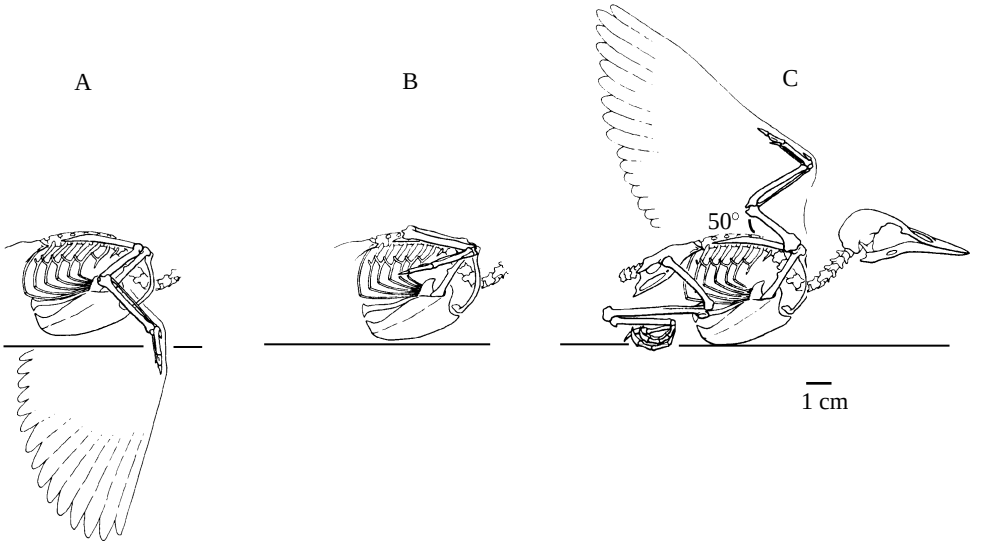

Fig. 3. General kinematics of wing upstroke of the European starling in lateral view. Data are based on a cinematographic analysis of an adult bird flying at 8 m s^{-1} in a wind tunnel (after Jenkins *et al.* 1988). (A) Downstroke–upstroke transition; (B) mid-upstroke; (C) upstroke–downstroke transition. The downstroke–upstroke transition is characterized by initiation of retraction, elevation and rotation of the humerus, flexion of the elbow and flexion/supination of the carpometacarpus (wrist). By mid-upstroke, the humerus is maximally retracted and the elbow and wrist are maximally flexed. Late upstroke is characterized by protraction/elevation of the humerus and extension of the elbow and wrist. Humeral elevation, as seen in lateral view, is typically 40–60 ° above the horizontal.

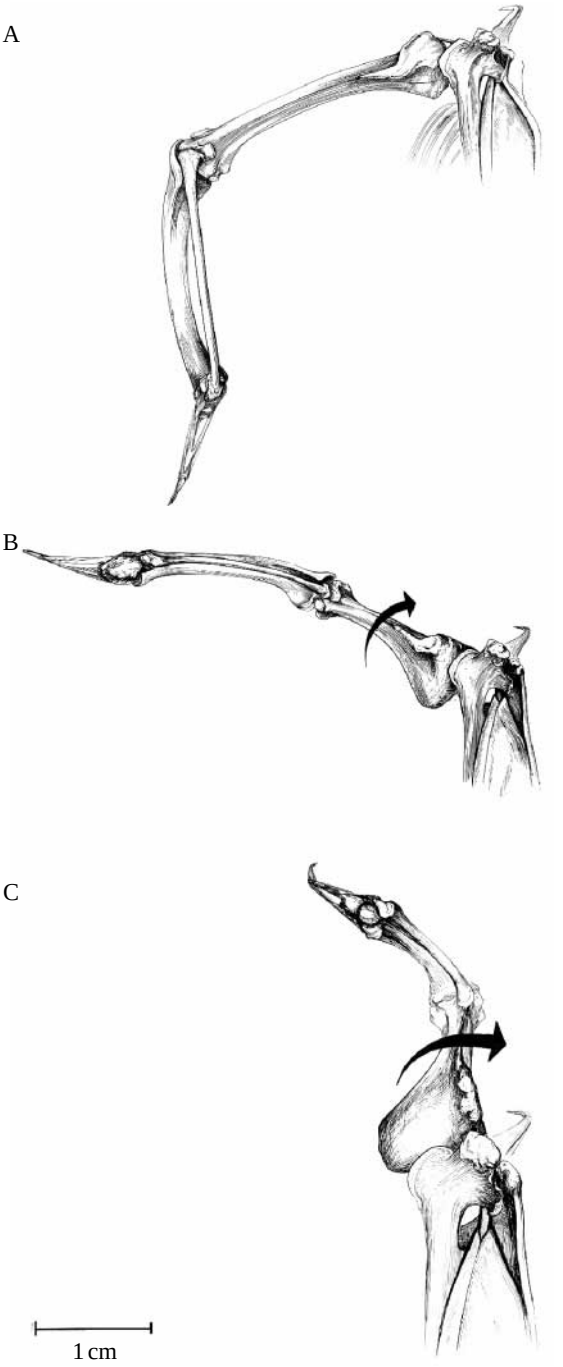

Fig. 4. Frontal view of a European starling in three positions of the flight cycle during upstroke; renderings based on cinematographic records and *in situ* stimulation of the SC. (A) Downstroke–upstroke transition; (B) mid-upstroke; (C) late upstroke. At the downstroke–upstroke transition, the humerus may be depressed by 10–20 ° below the horizontal as it begins its retraction, rotation and elevation. By mid-upstroke, the humerus is fully retracted, rotating rapidly and parallel to the horizontal. By late upstroke, the humerus has rotated through 70–80 ° (note the translation of the ect-epicondyles, ent-epicondyles and deltopectoral crest of the humerus), elevated to its maximum of 40–60 ° and protracted to its full extent of 50–60 °. These simultaneous retraction/protraction, rotation and elevation movements of the humerus serve to reposition the wing's ventral surface laterally for the following downstroke.

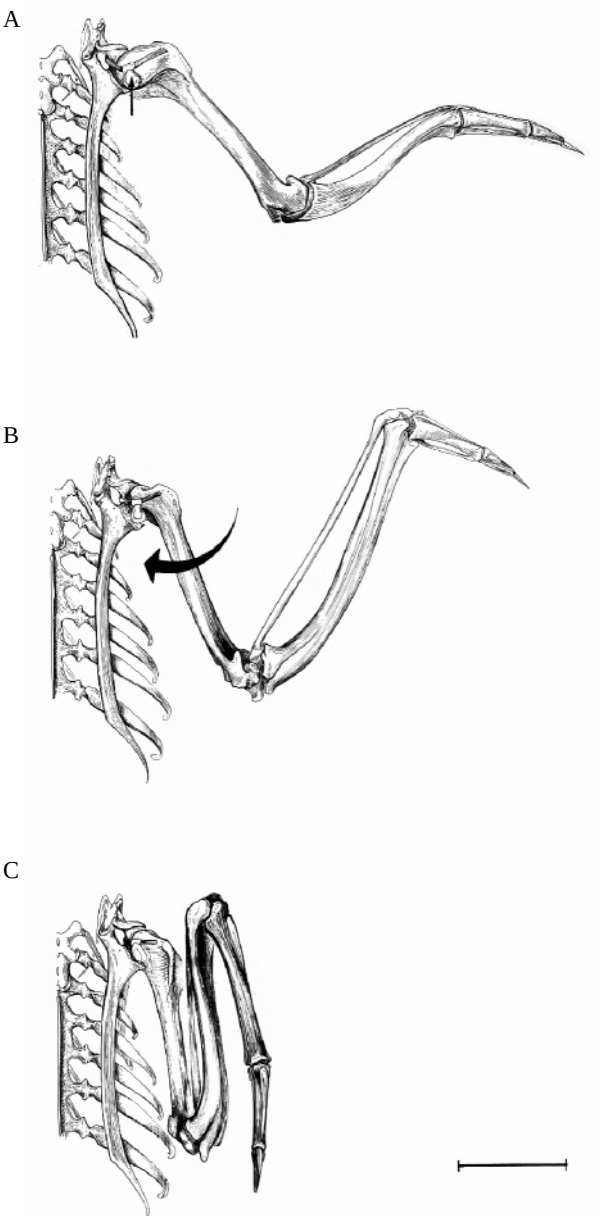

Fig. 5. Dorsal view of the right wing of an adult European starling in three positions during the upstroke. (A) Downstroke–upstroke transition; (B) mid-upstroke; (C) late upstroke. A small sesamoid bone, the Os humerocapsularis (small arrow), slings the tendon of the SC and maintains an acute angle of insertion medially. The instantaneous angle of retraction/protraction of the humerus during upstroke has a profound effect on wing kinematics. A retracted position of the humerus as it is elevated into the parasagittal plane, characteristic for starlings, pigeons and many other modern flying birds, requires the humerus be rotated about its longitudinal axis (arrow in B) in order to position the wing's ventral surface laterally for the downstroke that follows. For details of the Os humerocapsularis, see Fig. 3 in Dial *et al.* (1991).

it begins its retraction, rotation and elevation (Figs 4A, 5A). By mid-upstroke, the humerus is fully retracted, rotating rapidly and is parallel to the horizontal (Figs 4B, 5B). By late upstroke, the humerus has rotated through 70–80 ° (note the

translation of the ect-epicondyles, ent-epicondyles and deltopectoral crest of the humerus, Figs 4, 5), is maximally elevated (50–60 °) and is fully protracted (50–60 °) (Figs 4C, 5C). The instantaneous angle of retraction/protraction of the humerus during upstroke has a profound effect on wing kinematics. If, for example, the humerus projected at a right angle from the bird's longitudinal axis at mid-upstroke and was elevated 90 ° into the parasagittal plane, the wing's ventral surface would face laterally, the position appropriate for the upstroke–downstroke transition. If at mid-upstroke the humerus is retracted to any extent, however, as is the case for starlings, pigeons and many other modern flying birds, simple elevation even through a full 90 °, will not position the wing's ventral surface appropriately; the surface faces posterolaterally, not laterally. In order to correct this, rotation of the humerus about its long axis must also occur to an extent that is dependent on the angle of retraction at the upstroke–downstroke transition.

Non-reduced preparations

We observed full rotation of the humerus into the parasagittal plane and elevations of 50–60 ° (in lateral view) in pigeons during stimulation of the SC. In these preparations, stimulation not only pulled the humeral axis into the parasagittal plane but drew its distal end across the mid-vertebral axis to the contralateral side.

In the non-reduced starling preparation, in contrast, although elevation/rotation occurred at stimulation, the humerus was not fully rotated into the parasagittal plane. During stimulation in this species, the humerus also protracted in late upstroke, which appeared to limit the extent of its rotation. As a result, the apparent angle of elevation in lateral view was 60 °, but the angle formed by the longitudinal axis of the humerus and the horizontal (in frontal view) was not as great as might be expected, approximately 60 °. When we retracted the elbow by 10–20 ° during stimulation (top of the upstroke position), however, the humerus did roll into the parasagittal plane. Movement of the distal humerus across the bird's midline was not observed in this species.

In each of the non-reduced preparations, we carried out an additional test by simultaneously providing moderate intramuscular stimulation through percutaneous electrodes to the sternobrachialis portion of the pectoralis as we stimulated the SC. In the pigeon, if the humerus was retracted to an angle of 40 ° or less, the results for humeral translation were as reported above. If the angle was greater than 40 °, however, the humerus was elevated at a steep angle (to approximately 80 °) with little humeral rotation.

Reduced preparations

Stimulation of the SC in pigeons and starlings resulted in limited elevation of the humerus; 55–60 ° and 45–50 °, respectively. In addition to rotation and elevation in the starling, we observed protraction of the humerus during stimulation. Protraction is facilitated by the angle of the muscle's tendon of insertion and of the surfaces of attachment on the anteromedial margin of the proximal humerus (Fig. 5A; see also Figs 3 and 4 in Dial *et al.* 1991). In starlings, the protractive force acts to elevate the distal humerus after its rotation into the parasagittal plane and contributes to its elevation.

Isometric forces of elevation and rotation

The SC elevates and rotates the humerus, but its relative contribution to rotation about its longitudinal axis is greatest (Table 1). The forces of elevation measured at the mid-shaft of the humerus coincident with the downstroke–upstroke transition and the mid-upstroke positions for a representative starling (starling 1, Table 1) were 0.94 N and 0.60 N, respectively (Fig. 6). For a representative pigeon (pigeon 1, Table 1), values of 9.3 N and 8.3 N, respectively, were recorded at these two wing positions (Fig. 6). We observed rotational forces at the center of the deltopectoral crest at the two kinematic positions of 5.6 N and 4.6 N, respectively, for starling 1 and 26.1 N and 32.1 N, respectively, for pigeon 1 (Table 1; Fig. 6).

The measured mid-shaft elevational forces are higher than those actually acting at the wing's center of mass. We used the laws of proportionality, the mid-shaft force and appropriate lever arm lengths to estimate these actual forces of elevation. In starling 1 and pigeon 1, for example, the corrected forces of elevation at the downstroke–upstroke transition were 0.4 N and 2.7 N, respectively, forces estimated to be 43 % and 30 % of the respective measured mid-shaft values (Table 1).

Length–force relationships

Active length–force curves

Fig. 7A,B illustrates the active and passive length–force curves for the SC muscle of the starling and pigeon. 'Zero' on the abscissa corresponds to the length where measured passive tension is zero. The length from zero to the length where maximal twitch force was measured is 5.0 mm for the starling and 8.0 mm for the pigeon. The ascending limb of the active curve for both species rises rapidly with length change, particularly for the starling. The increase in active force for each millimeter of length change in this species is almost 20 %

Table 1. *Action of the M. supracoracoideus in reduced preparations of pigeons and starlings*

	Elevational force (N)		Rotational force (N)	
	DS-US	M-US	DS-US	M-US
Starling 1	0.94 (0.40)	0.60 (0.29)	4.2	4.0
Starling 2	0.89 (0.35)	0.42 (0.19)	5.6	4.6
Pigeon 1	9.30 (2.7)	8.30 (2.4)	26.10	32.10
Pigeon 2	6.60 (2.0)	8.70 (2.6)	21.50	17.80

DS-US, downstroke–upstroke transition; M-US, mid-upstroke.

Elevational force was measured at the mid-shaft of humerus. Values in parentheses represent the force at the wing's center of mass estimated using known force/lever proportionality.

of the maximum active force over the range 0–4.0 mm (Fig. 7A). For the pigeon, active force increases by approximately 10 % of the maximum per millimeter over the range 0–8 mm. The steepness of the curves is in part a function of the bipinnate structure of the SC and its short, obliquely oriented fascicles. When the length–force relationship is expressed as a function of the angle of depression/elevation of the humerus (the angle in lateral view of the long axis of humerus and the scapula), it is evident that both species operate on the ascending arm of the length–force curve (Fig. 8A,B). The downstroke–upstroke transition (at −20 °, starling; estimated −20 °, pigeon, in Fig. 8) is near the peak of the active length–force curve for both species.

Maximal tetanic forces were 6.5±1.2 N for starlings (N=4) and 39.4±6.2 N for pigeons (N=6) (mean ± S.D.).

Passive length–force curves

Mean (± S.E.M.) passive force values at maximum *in situ* length were 1.0±0.10 N for the starling (N=4) and 5.0±2.0±0.45 N for the pigeon (N=8) (Fig. 7A,B). When these absolute values are expressed as a percentage of the active twitch force, the passive force for the starling SC is 30 % of the maximum active force and that for the pigeon is 10 % of the maximum active force.

The comparative series elasticity of the two musculotendinous complexes is unknown but, if they are comparable, the relationship between the profile of the passive length–force and the active length–force curves we measured suggests that the starling SC is a relatively stiffer muscle than that of the pigeon.

Discussion

The results contained in this report address the mechanical contractile properties of the M. supracoracoideus (SC) of two species of birds with contrasting flight styles. Many other studies of the relationship between isometric muscle contractile properties and muscle length are concerned largely with either the underlying properties of the contractile machinery and its arrangement within sarcomeres (Gordon *et al.* 1966*a*,*b*; Keurs *et al.* 1978; Rack and Westbury, 1969) or the effects of muscle architecture on the shape of the active length–force curve (for a review, see Ettema and Huijing, 1994). The present study, however, relates to the more general issues of neural control and the evolution of neuroanatomical and musculoskeletal systems of locomotion. An underlying assumption is that the anatomical arrangement and fascicle organization of the SC in all birds capable of sustained flapping flight reflects an evolutionary response to the functional demands of powered flight. Thus, emphasis is placed upon the action of the SC during wing movements in birds and its role in the evolution of powered flight.

We used as a reference for our physiological measurements the wing kinematics for European starlings flying in a wind tunnel reported in the cineradiographic study of Dial *et al.* (1991). Kinematic data of comparable precision are not available for the pigeon; we made estimates from Brown (1951) and Simpson (1983) and from isolated sequences of pigeons in flight recorded on 16 mm film at 1000 frames s^{-1} for

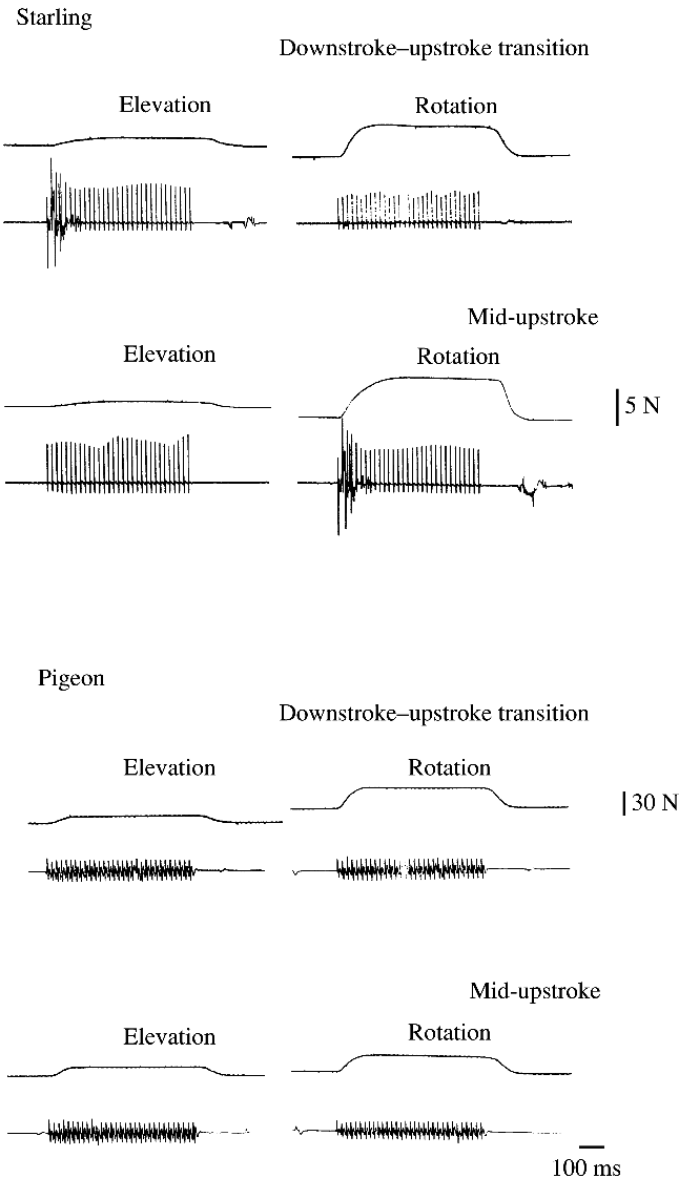

Fig. 6. Isometric *in situ* forces of elevation and rotation of the SC for the European starling and pigeon. We measured the elevational force at the mid-shaft of the humerus and the rotational force at the deltopectoral crest with the wing joint angles set to coincide with those for the downstroke–upstroke transition and mid-upstroke. The starling is 'Starling 1' and the pigeon is 'Pigeon 1' of Table 1. In all cases, the muscle nerve was stimulated tetanically (0.2 ms pulse duration, 60 Hz, 500 ms train duration) and isometric force was recorded. Force is the upper trace; electromyogram activity is the lower trace. The mid-shaft forces of elevation shown here were corrected to give a more appropriate estimation of the force of elevation applied at the wing's center of mass and are reported in Table 1. The force of elevation produced by the SC on the humerus is substantially lower than the force of rotation produced about its longitudinal axis.

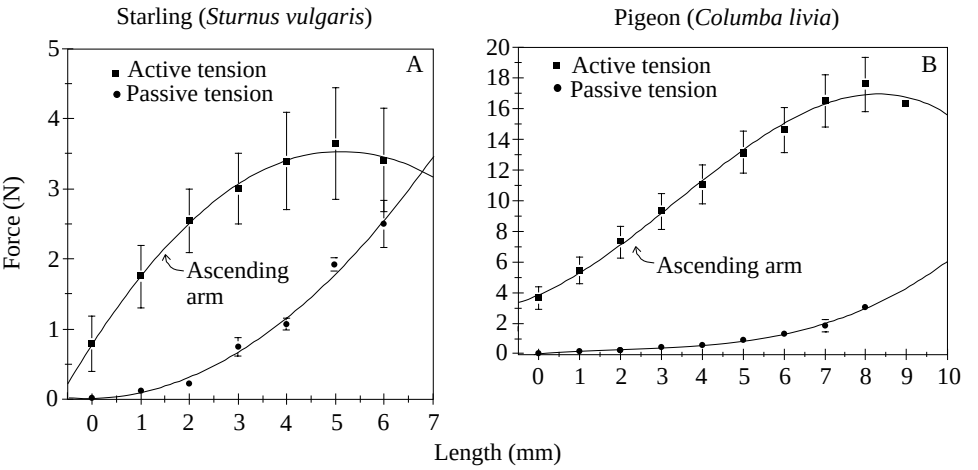

Fig. 7. Total active and passive isometric force of the SC as a function of relative muscle length for the European starling (A) and the pigeon (B). Active length–force curves were derived over a 5 mm length change for the starling and a 12 mm length change for the pigeon by eliciting twitch responses (single, supramaximal stimulation; 0.2 ms pulse duration) at a series of lengths encompassing the muscles' normal excursion range. All points shown represent mean twitch force (± S.E.M., starlings, N=4; pigeons, N=8) at each length and are separated by 1.0 mm increments. The length from the point of zero passive tension to the length of maximal active twitch force is 5.0 mm for the starling and 8.0 mm for the pigeon. Expressed as a percentage, the starling SC displays a 20 % increase in active force production for each millimeter of length change over the range 0–4.0 mm. For the pigeon, active force increases by approximately 10 % for each millimeter over the range 0–8.0 mm. The ascending limb of the active length–force curves for both species is steep, in part a function of the short and oblique fascicles associated with the bipinnate architecture of the SC. The passive curves are relatively steep, particularly for the starling for which the maximum active twitch force increases by 10 % for each 1.0 mm of length change. At the peak of the active curve in this species, passive force is approximately 50 % of the maximum active twitch force.

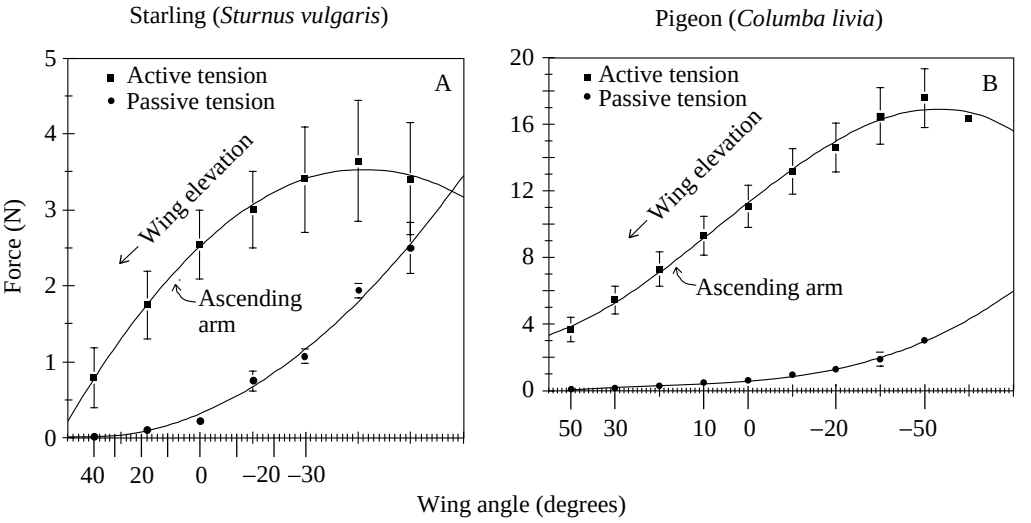

Fig. 8. Total isometric length–force curves of the SC as a function of angle of humeral elevation for the European starling (A) and the pigeon (B). For both species, the muscle functions on the ascending limb of the active length–force curve, not on the plateau. The peak of active force occurs near the downstroke–upstroke transition (wing angle –20 ° for both species), the length at which the muscle produces the maximum twitch force. During upstroke, as the humerus elevates and rotates, the potential for active force production by the SC decreases. Angle of elevation was derived from absolute muscle length as described in Materials and methods.

a previous study (Goslow, 1972). The downstroke–upstroke transition in both species begins with the humerus below the horizontal and is characterized by a rapid sequence of events including simultaneous retraction, rotation and elevation of the humerus, rapid flexion of the elbow and rapid flexion/supination of the wrist.

Functional implications of the length–force relationships

Active length–force curves

The working range of the SC in both species corresponds to the ascending limb of the active length–force curve. The potential for greatest active force is high on the ascending limb at joint angles coincident with the downstroke–upstroke transition, a time when the humerus is depressed below the horizontal and rotated maximally forward. As the muscle shortens to counterrotate and elevate the humerus during early upstroke, the potential for active force at shorter lengths declines at a relatively rapid rate.

A working range restricted to the ascending limb of the curve is consistent with reports for many, but not all, locomotor muscles for which direct length–force measurements have been made. Muscle use on the ascending limb, for example, was reported for three of four shoulder muscles of the savannah monitor lizard (*Varanus exanthematicus*) (Young *et al.* 1990) and for all ankle extensor muscles of the striped skunk (*Mephitis mephitis*) walking at two speeds (Goslow and Van

De Graff, 1982). Stephens *et al.* (1975) reported similar usage of the medial gastrocnemius of cats during walking and trotting, and Goslow (1972) reported the same for several hindlimb muscles in raptorial birds during their striking and grasping behavior. There is evidence, however, that individual muscles may alter their working range depending on the locomotor task and that muscle groups within a species may be differentially 'specialized' for work along a particular region of the length–force curve. Stephens *et al.* (1975) noted that when a cat gallops, a more vigorous locomotor behavior than walking and trotting, the medial gastrocnemius is used higher on the ascending limb of the length–force curve. In jumping cats, a ballistic movement considered maximal for the species, Zajac (1985) used theoretically computed sarcomere length–force curves based on muscle geometry, fiber architecture and joint angle trajectories, and correlated them with electromyographic activity for seven hindlimb muscles. His calculations revealed that one of the seven muscles functions on the plateau and the others remain restricted to the ascending limb of the sarcomere length–force curve, thus producing below maximal force. In other similar studies of sarcomere length changes, the swimming muscles of fishes have been reported to operate on the plateau (Lieber *et al.* 1992; Rome and Sosnicki, 1991) and frog hindlimb muscles on the ascending limb (Mai and Lieber, 1990; Lieber and Brown, 1992) and plateau (Lutz and Rome, 1994) of the curve. Loren *et al.* (1996) recently reported that human wrist flexors work primarily on the ascending limb, whereas wrist extensors contract predominantly on the plateau region.

In our estimation, humeral excursions during take-off, landing and hovering flight in starlings and pigeons are more extensive than during level flight, but the data with which to assess this are not yet available. If so, contractions of the SC during these maneuvers might occur at longer lengths which approach the plateau of the curve. There are indirect data to support this idea. A diffraction study to determine the minimum and maximum sarcomere lengths in two species of birds, the budgerigar (*Melopsittacus undulatus*) and zebra finch (*Taeniopygia guttata*), predicted that the SC and pectoralis muscles work on the ascending limb as well as the plateau of their respective length–force curves (Cutts, 1986). An earlier investigation of fast and slow muscle in the chicken, in which sarcomere lengths and contractile properties were correlated (Page, 1969), formed the basis for Cutts' calculations. This conclusion must be treated with caution, however, because of the difficulty of consistently predicting a whole muscle's length–force curve on the basis of the curve for isolated fibers or sarcomeres (for a review, see Kardel, 1990; Ettema and Huijing, 1994; Ettema, 1996) and in the light of recent revelations concerning the apparent in-series organization of many avian muscles (Gaunt and Gans, 1993; Trotter *et al.* 1992).

Multiple structural, functional and phylogenetic factors must interact to determine where on the length–force curve a specific muscle works. Data that relate to muscle injury in humans have also been advanced to explain why a muscle's design enables it to work on the ascending limb but not the plateau and descending arm of the length–force curve (Fridén and Lieber, 1992).

Passive length–force curves

The presence of a significant passive force in the SC of starlings may contribute to wing elevation or humeral stabilization when the bird is at rest. In both species, increasing passive tension with humeral depression is presumably available to enhance wing deceleration/acceleration at the downstroke–upstroke transition. Most of the passive force in vertebrate muscle is thought to be exerted by forces intrinsic to the resting sarcomere (Magid and Law, 1985). Experimental studies of the contribution of the endomysium to passive force have focused primarily on the mechanical stiffness of this complex for single muscle fibers (for a review, see Trotter *et al.* 1995). These experimental data and analyses of the endomysium using models (Purslow and Trotter, 1994) suggest that, because muscles can produce high isometric forces at their optimal length, the endomysium, with its relatively low tensile stiffness at that length and even longer lengths, contributes little to the longitudinal forces produced by the associated contracting fibers. Our active force curves (Figs 7, 8) are for isometric twitch not tetanus, and when the maximum mean tetanic forces for the SC are considered (6.5 N for starling; 39.4 N for pigeon), it is evident that the passive component is relatively small, particularly for the pigeon.

There is indirect evidence from neuromuscular endplate staining patterns, however, that the muscle fibers within the SC of starlings and pigeons, as well as other species of birds, are organized in series (Gaunt and Gans, 1993). Microdissection of individual fibers within the SC is necessary for confirmation of this organization. Nevertheless, for in-series muscles which contain fibers that do not traverse the entire origin-to-insertion length and do not contain myomous junctions for end-to-end force transmission, the endomysium has been implicated in the transmission of shear forces from one fiber to the next as the way in which forces are distributed from origin to insertion (Purslow and Trotter, 1994; Trotter, 1993; Trotter and Purslow, 1992). If this is the case, the passive tension component may indeed be mechanically important to the function of the SC *in vivo*.

If there is a functional explanation for the presence of a stiffer SC in starlings than in pigeons, it is elusive. It is, of course, attractive to think that additional passive stiffness may relate to contractile frequency and contribute to the execution and/or energetics of the higher-frequency oscillations of the wing characteristic of starlings. Passive length–force curves that show stiffer muscle characteristics have also been reported for the Mm. biceps brachii, pectoralis and supracoracoideus of the monitor lizard *Varanus exanthematicus* (Young *et al.* 1990), as well as for rat papillary muscle (Layland *et al.* 1995). A commonality in function of these muscles is not immediately apparent and underscores the need for additional comparative data.

Whole-muscle performance in flight

The maximal isometric forces recorded in this study are used

for comparative purposes and are considered to reflect the potential forces, not necessarily the real forces, used by naturally behaving birds in flight. The length–force relationship is considered to be the consequence of both 'physical' and 'activation' factors which are influenced by instantaneous as well as by changing muscle length (Edman *et al.* 1976; Gordon *et al.* 1966*a*,*b*; Jewell and Wilkie, 1958; Joyce and Rack, 1969; Joyce *et al.* 1969; Katz, 1939). As the muscle shortens (upstroke), force production at any given length is less than it would be during isometric contraction owing to force–velocity properties, but during an eccentric contraction (late downstroke) the force sustained by the muscle may increase substantially above isometric values (Alexander and Bennet-Clark, 1977; Cavagna *et al.* 1968).

Information about the state of the SC's force coupled with its instantaneous length throughout a wingbeat is important in order to document fully the muscle's behavioral dynamics and contribution to each upstroke. An *in vivo* profile of force and length for the SC is not yet available for any bird species, however, but some predictions can be made. Neural activation of the SC, as reflected by electromyographic studies of starlings flying in a wind tunnel (Dial *et al.* 1991) and pigeons in free flight (Dial *et al.* 1988), begins in late downstroke and ends prior to the upstroke–downstroke transition. These electrically active periods are not instantaneously coincident in time with force production because of an electromechanical delay (Goslow and Dial, 1990). Direct measurements of this delay in the pectoralis of starlings and pigeons in flight, as determined by simultaneous electromyography (EMG) and bone strain measurements (Biewener *et al.* 1992; Dial and Biewener, 1993), reveal the latency between electrical activity and force initiation to be short (3–5 ms and 6–7 ms, respectively); the longest value reported was 8.0 ms for pigeons at take-off. Once initiated, the force produced by the pectoralis on the humeral deltopectoral crest increases from late upstroke through the upstroke–downstroke transition and peaks 5 and 8 ms (starling and pigeon, respectively) after electrical activity ceases, lasting 1.4 times the duration of the EMG burst. On the basis of these observations, it was concluded that residual force in the pectoralis may overlap the rising force of the SC at the downstroke–upstroke transition.

Opposing forces in the pectoralis and SC by their co-contraction at the wing turnaround positions has intuitive appeal; the inertial properties of a rapidly oscillating limb can best be controlled in this way. Co-contraction also provides the possibility of subtle adjustments of the wing not possible by two antagonists working independently. Our observations that humeral movements are dependent upon initial wing position and/or levels of SC and pectoralis co-activation *in situ* attest to this and lead us to speculate how their co-contraction *in vivo* augments the neural control of the shoulder. We present a hypothetical case of SC and pectoralis co-contraction during the wingbeat cycle as an illustration (Fig. 9).

Dial and Biewener (1993) presented 'representative' EMG and bone strain/muscle force recordings for the pectoralis of pigeons during take-off, landing, near-vertical ascent/descent and level flight. The profile of the strain/force trace remained relatively consistent for all these flight modes, and some variation in the level (magnitude) of strain at the downstroke–upstroke transition was noted. Although a correlation between residual strain and flight mode was not demonstrated, it might be expected that during the wing movements of flight, particularly those necessary for the control of non-level flight (rolling, pitching, yawing), the extent of antagonistic force overlap would vary with neural modulation. A generic strain/force curve for the pectoralis in starlings and pigeons during flight (after Biewener *et al.* 1991; Dial and Biewener, 1993), coupled with a hypothetical curve for the SC, reveals their potential *in vivo* interaction (Fig. 9).

The hypothetical force curve for the SC is estimated from its contractile and architectural properties. Within each species, the SC and pectoralis possess similar twitch contraction times. For starlings (N=10) and pigeons (N=10), we recorded mean twitch contraction times for the SC of 45 ms and 50 ms, respectively, values that are similar to or the same as those reported for their respective pectoralis muscles (starling, Goslow and Dial, 1990; pigeon, A. Sokoloff and G. E. Goslow, Jr, unpublished observations). In addition, the two antagonists possess a bipinnate fascicle architecture in each species. However, there are considerable differences in fascicle length

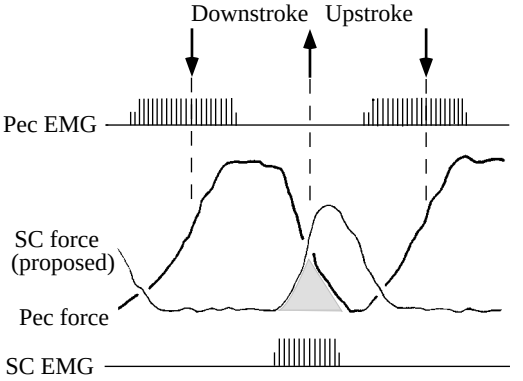

Fig. 9. Proposed hypothetical co-contraction of two antagonists for enhanced wing control. Diagrammatic electromyograms (EMG) and muscle force profiles for the M. pectoralis (Pec) and M. supracoracoideus (SC) during a single wingbeat. The downward-pointing arrow (↓) represents the onset of downstroke, the upward-pointing arrow (↑) represents the onset of upstroke. Peak muscle force in the pectoralis occurs after EMG offset and declines variably during late downstroke. The extent to which pectoralis force continues into the subsequent early upstroke is predicted to vary with flight mode and/or extraneous perturbations. We predict that force in the relatively 'stiff' SC will rise rapidly during the period of co-contraction with the pectoralis at the downstroke–upstroke transition. As the humerus rotates and elevates during the ensuing middle-to-late upstroke, force in the SC will fall rapidly. The potential for co-contraction at the downstroke–upstroke transition (shaded area) suggests that this is the time during the wingbeat cycle at which neural modulation of the wing stroke is most effective. Pectoralis EMG and force profile after Biewener *et al.* (1992) and Dial and Biewener (1993); SC EMG pattern after Dial *et al.* (1988, 1991).

and moment arm distance from the glenohumeral joint between the two muscles; the fascicles and moment arm of the SC are relatively short. Taken collectively, these properties suggest that the SC presents a relatively 'stiff' complex during the late downstroke/early upstroke period, which results in a rapid increase in the muscle's force (high stress) but little length change (low strain). The effect on the humerus is an abrupt, rapid force increase which overlaps to some extent the declining force of the pectoralis (Fig. 9). As the humerus rotates and elevates during the ensuing mid- and late upstroke, we estimate that active force in the SC falls precipitously (low stress) as the muscle shortens rapidly (high strain). We anticipate that co-contraction of the two antagonists at the time of downstroke–upstroke transition (shaded area, Fig. 9) may be an opportune time for neuromuscular adjustments of shoulder kinematics to meet the demands of flight. Whether this is true at the upstroke–downstroke transition is more difficult to predict and awaits either direct measurements of the force profile of the SC *in vivo* or information about the muscle's force–velocity characteristics.

A case for humeral rotation

The bipinnate structure of the SC with its relatively short but numerous fascicles, characteristic of all birds we examined, is an architecture suitable for the production of high force but limited excursion. We measured maximal tetanic forces of the SC in both species of 7–10 times body weight; a significant force for a muscle conventionally considered to be non-propulsive. The SC's moment arm for humeral rotation is short; we estimate its maximum in the starling to be 2 mm and in the pigeon 4 mm. Although the mechanical advantage of the SC is low, its high input force, particularly at the downstroke–upstroke transition, is favorable for the production of high-velocity movements at the distal wing. Our *in situ* excursion and force measurements in the reduced and non-reduced preparations reveal the primary role of the SC in starlings and pigeons to be forceful, high-velocity long-axis rotation of the humerus and a secondary role of limited wing elevation. Retraction of the humerus and flexion of the elbow and wrist at early upstroke bring the wing's center of gravity closer to the body, which improves the SC's mechanical advantage for both actions. These general kinematics were reported for pigeons during 'propulsive' and 'non-propulsive' upstrokes associated with slow and fast flight (Brown, 1951) and take-off (Simpson, 1983). Dial *et al.* (1991) reported more precisely for starlings that during early upstroke the elbow flexes by 75 ° and the wrist flexes by 100 ° in 40 ms, rates that exceed any reported values for limb movements in vertebrates. The humerus at this same time is retracted by 20 ° in 15 ms, a movement that also improves the SC's ability to rotate the humerus about its longitudinal axis. It should be noted that marked supination (circumflexion) of the hand also characterizes early upstroke.

The translation of humeral rotation into wing tip elevation is strongly dependent upon the orientation of the humerus to the longitudinal axis of the body (Ostrom *et al.* 1997). When viewed from above (in dorsal view), the angle formed by the long axis of the humerus and the bird's longitudinal axis when the wing is at the upstroke–downstroke transition position is not 90 ° as might be expected, but is retracted to form an acute angle. Elevation of a humerus oriented at near 90 ° to the parasagittal plane requires an elevator muscle(s) capable of shortening a long excursion. When the humerus is retracted, however, its rotation translates into an elevation of the wing's leading edge. At the upstroke–downstroke transition in starlings, for example, the angle of humeral retraction is at its maximum of 55–60 ° and during early upstroke decreases to its minimum of 25–30 ° (i.e. the humerus is progressively retracted) (Fig. 5). Simple elevation of a retracted humerus results in the wing's ventral surface facing posterolaterally instead of the more functional lateral position, whereas a simultaneous rotation and elevation of the humerus in early upstroke orients the hand and forearm so that their extension during late upstroke orients the fully outstretched wing in the parasagittal plane; i.e. the wing's ventral surface faces laterally. Humeral rotation/retraction as described here is the key to the execution of the high-amplitude, high-frequency wingbeats used by so many birds and may be important to long-winged forms as well. In a study of the shoulder of the Cretaceous pterodactyloid pterosaur *Santanadactylus brasilensis*, with an estimated body mass of 3.9–7.3 kg and total wingspan of 4.7 m, Hazlehurst and Rayner (1992) propose humeral rotation to be the key to wing elevation in this species. Study of the articular surfaces of the proximal humerus and glenoid revealed a limited ability for humeral depression/elevation at that joint, but when humeral rotation at even modest angles of retraction was estimated, a mechanism for wing elevation was determined. For example, 70 ° of longitudinal rotation of the humerus held at an angle to the body axis of 75 ° (their 15 ° angle behind the transverse axis of the body), results in a wing tip elevation of 0 °, whereas the same rotation at a retraction angle of 65 ° elevates the wing tip by 11.4 °.

We believe that the failure of stimulation of the SC in the non-reduced starling preparation to rotate the humerus fully into the parasagittal plane was due to its simultaneous protraction effect on the humerus in the late-upstroke position. This view is supported by the observation that slight retraction applied externally to the distal humerus during stimulation resulted in full rotation of the bone into the parasagittal plane. This emphasizes again that the SC does not act in isolation during flight, but that co-contractions of other muscles also play a role in determining this muscle's precise action. For example, to achieve the kinematic position demonstrated by starlings at the end of upstroke (Fig. 3C), a co-contraction of the M. scapulotriceps along with the SC may be required. Dial *et al.* (1991) reported that the M. scapulotriceps, a muscle that takes its anatomical origin from the scapula, was electrically active from mid-upstroke to early downstroke – an unusual pattern in this muscle for tetrapods. By inferred force production, they proposed that the muscle may serve not only to stabilize the elbow but also to retract the humerus in late

upstroke. If the force were high enough to counter the protractive force of the SC, such retraction might augment the ability of the SC to rotate the humerus fully.

The outstretched wing position in the parasagittal plane at the beginning of the power stroke characteristic of starlings and pigeons is the result not only of the action of the SC but also of the structurally derived avian shoulder joint. The avian glenoid, formed by the coracoid anteriorly and scapula posteriorly, is a hemisellar (half-saddle) joint. The joint's surface is concavoconvex in configuration, faces dorsolaterally and articulates with a bulbous humeral head. Jenkins (1993) used the starling as representative of a species capable of powered flight and reviewed the evolution of this joint in a comparative study, providing a new interpretation of its functional morphology and evolutionary significance based on a cineradiographic analysis of the wingbeat cycle. The articulation of the humeral head on the dorsally facing surface of the glenoid, the labrum cavitatis glenoidalis, is the glenoid feature which allows for full abduction of the wing into the parasagittal plane late in the upstroke.

Additional evidence to support our interpretation of a long-axis rotational role for the SC comes from its electrical activity pattern during flapping flight in several species of birds with diverse wing morphologies. Aerodynamic models, based most recently on flow visualization techniques for the identification of momentum flow from the wing, predict that active muscle contractile force is required for wing elevation in many birds during slow, steady flight, particularly in those species with short wings (Rayner, 1985). Flow visualization studies of two small passerines, the chaffinch (*Fringilla coelebs*) and brambling (*F. montifringilla*) (Kokshaysky, 1979), and studies of jackdaws (*Corvus monedula*) (Spedding, 1986) and pigeons (Spedding *et al.* 1984) during slow flight reveal a pattern of wake vortices which form a series of closed vortex rings behind each wing during each wingbeat cycle (the 'vortex ring gait'; Rayner, 1988). Whether birds with short wings continue to use a vortex ring gait at their fast flight speeds remains to be determined. Consistent with a requirement for muscle force during wing elevation in short-winged forms, EMG activity of the SC at several flight speeds for pigeons (Dial *et al.* 1988), starlings (Dial *et al.* 1991) and budgerigars (Tobalske and Dial, 1994) has been reported. In contrast to these short-winged species, however, Spedding (1987) illustrated that the kestrel (*Falco tinnunculus*), a species with a relatively long wing with a high aspect ratio, sheds a continuous vortex from each wing when flying at relatively fast cruising speeds (the 'continuous vortex gait'; Rayner, 1988). The continuous vortex pattern, as opposed to the vortex ring pattern, reveals the upstroke to be aerodynamically active when weight is supported but thrust is negative. During such a continuous vortex gait, it is predicted that muscle force during upstroke is not required since aerodynamic lift should be sufficient (Rayner, 1985). In an electromyographic/cinematographic study of the American kestral (*Falco sparverius*) flying in a wind tunnel at a range of forward speeds, however, Meyers (1993) recorded EMG activity from the SC at all flapping speeds. It is acknowledged that EMG activity does not necessarily correlate with useful mechanical force (Spector *et al.* 1980) and that its presence may reflect outflow modulation of a central neural control program (Cohen *et al.* 1988). Alternatively, as we believe, the activity of the SC at high flight speeds in these short-winged species as well as several speeds in the long-winged species reflects its contribution to humeral rotation.

Sy (1936) described humeral axial rotation as a mechanism for the execution of wing upstroke in pigeons and generalized its importance for other relatively small birds possessing powered flight. His experiments to illustrate this point, however, are not fully appreciated. Sy (1936) is most often cited in discussions of the evolution of powered flight for his observations that pigeons with bilateral tenotomy of the SC are capable of flight, but cannot take off from the ground. Perhaps less appreciated was Sy's (1936) identical procedure on at least one adult crow *Corvus corax* for which he reported not only normal take-off but normal flight. In his discussion of the crow, however, Sy alludes that the crow was limited in its flight duration (Sy, 1936, page 232). Sokoloff *et al.* (1994), in a cinematographic and electromyographic analysis of adult starlings, bilaterally denervated (N=4) or tenotomized (N=2) the SC and reported that all the birds but one could take off, *but not without difficulty*. The importance of this observation, that the flight capabilities of these deprived birds is not normal, for placing Sy's (1936) original study into perspective cannot be overemphasized. In our estimation, the extent of impairment incurred by the loss of the SC for different species is a function of wing loading (body weight/wing area), of the mechanical organization of the SC or of some combination of these. We believe that the impaired take-off capability of birds deprived of a functional SC relates to their inability to rotate the humerus rapidly on its long axis.

Evolution of the derived M. supracoracoideus

The early fossil record of birds since the Jurassic demonstrates a number of advanced characteristics that signal an evolutionary progression towards powered flight. For example, the glenoid of *Archaeopteryx* and *Sinornis* faces laterally (Jenkins, 1993; Martin, 1983; Ostrom, 1976*a*,*b*; Sereno and Rao, 1992), which limited extensive abduction of the wing into the parasagittal plane. The triosseal canal, formed variously by the dorsal extremities of the furcula and coracoid and the anterior extremity (acromium) of the scapula, provides a passage for the tendon of the SC to its insertion point on the dorsal aspect of the humerus and represents an advanced feature. In his extensive monograph on the anatomy of a diversity of birds capable of powered flight (and several flightless species), Fürbinger (1888) illustrated the triosseal canal of over 50 species. In the seven preserved specimens of the Jurassic bird *Archaeopteryx*, however, there is no evidence of a triosseal canal or of a derived SC with a dorsally inserting tendon (Ostrom, 1976*a*,*b*; Wellnhofer, 1988, 1993). In the recently described series of enantiornithine and non-enantiornithine Mesozoic birds (i.e. *Eoalulavis*, *Neuquenoris*, *Cathyornis*, *Concornis*, *Iberomesornis* and *Ambiortis*), the

presence of an elongated coracoid, furcula and scapular acromion suggests that a derived SC may have been present, although a triosseal canal has not been identified *de facto* (for a review, see Chiappe, 1995; Feduccia, 1995; Sanz *et al.* 1996). In a thoughtful discourse on the flight capabilities of *Archaeopteryx*, Ruben (1991) set out convincing arguments that, without the benefit of a highly derived SC for wing upstroke, an ectotherm could still produce enough power from its deltoid muscles to accomplish brief periods of powered flight. This may be true, but in extant birds the morphology of the deltoids does not appear to facilitate rapid or extensive long-axis rotation of the humerus. The lack of the triosseum/SC level of organization in the Jurassic and Mesozoic birds described thus far precludes a high-velocity recovery stroke like that present in modern birds which, in turn, would have limited their abilities for powered flight.

The humeral protraction about the glenohumeral joint that we observed in starlings during stimulation of the SC may also reflect an important functional advancement. This action may be useful at late upstroke or late downstroke. In many groups of birds capable of powered flight, when the humerus is adducted, the triosseal canal is positioned well forward of the external tuberosity. As noted for the starling, the movement produced after the humerus has rotated and moved into the parasagittal plane can be considered to be protraction (drawing the humeral axis away from the longitudinal axis of the body) and elevation (in lateral view).

Protraction of the wing during downstroke, particularly during slow flight, is a distinct kinematic event of powered flight in pigeons and starlings (Brown, 1951; Simpson, 1983; Dial *et al.* 1991). It has been shown in pigeons that the pectoralis fascicles which arise from the furcula are responsible for at least part of this protraction (Dial *et al.* 1988). Young *et al.* (1990) discussed the potential significance of this protractive pectoralis/furcula musculoskeletal complex to the origin of flapping flight. Our observations in the present study suggest that, in addition, the co-contraction of the SC and pectoralis at the downstroke–upstroke transition, when force in the pectoralis is waning and force in the SC is high (Fig. 9), may augment protraction in at least some species. It is difficult to assess the importance of these proposed actions to powered flight or to its evolution on the basis of the present data, but when a fossil bird is found which demonstrates a derived SC, the spatial configuration of the shoulder may offer some clues.

We have argued elsewhere that the ability of *Archaeopteryx* to supinate the manus automatically during wrist flexion was a significant advance in the evolution of powered flight (Ostrom *et al.* 1997). The wrist of *Archaeopteryx* possessed a semi-lunate carpal characterized by an asymmetrical ginglymus-like facet on its proximal surface (Ostrom, 1976*a*,*b*). This carpal, configured such that, upon wrist flexion, automatic supination of the hand occurs, is also present in several maniraptoran theropods (Ostrom, 1969). The homology of this semi-lunate carpal in modern birds is in doubt (for a review, see Ostrom 1995), but it is thought that its distal end (i.e. the end opposite the asymmetrical facet) is fused into the proximal end of the carpometacarpus. As a result, the asymmetrical ginglymus-like facet is now identified in modern birds as the trochlea carpalis of the proximal carpometacarpus. The trochlea carpalis is an asymmetrical surface which articulates proximately with an irregularly shaped wrist bone, the cuneiform, in such a way that, upon wrist flexion, automatic supination of the hand ensues (Vazquez, 1992).

It may be that supination in modern birds, so important to the execution of upstroke, followed a two-step process. Initially, some degree of supination occurred during wrist flexion as a result of the asymmetrical configuration of the semilunate carpal. With the subsequent evolution of a derived SC capable of imparting a large torque to the humerus, supination of the manus was augmented by the high-velocity rotation of the wing/hand, characteristic of modern birds capable of powered, flapping flight.

The ideas expressed in this manuscript were greatly clarified by discussions with various colleagues, particularly L. Chiappe and J. Ostrom, to whom we extend our sincere appreciation. Our thanks to C. Kovacs for his comments on a draft of the manuscript. For technical assistance and cheerful support during those late nights, we heartily acknowledge A. Valore-Caplan, K. Jackson and M. Morimoto. We thank L. L. Meszoly and K. Brown-Wing for rendering the illustrations (Figs 1 and 2, and Figs 4 and 5, respectively). Supported by NSF grant IBN 9220097.

References

ALEXANDER, R. MCN. AND BENNET-CLARK, H. C. (1977). Storage of elastic strain energy in muscle and other tissues. *Nature* **265**, 114–117.

BAUMEL, J. J. (1979). *Nomina Anatomica Avium.* London: Academic Press. 637pp.

BIEWENER, A. A., DIAL, K. P. AND GOSLOW, G. E., JR (1992). Pectoralis muscle force and power output during flight in the starling. *J. exp. Biol.* **164**, 1–18.

BROWN, R. H. J. (1951). Flapping flight. *Ibis* **93**, 335–359.

BROWN, R. H. J. (1963). The flight of birds. *Biol. Rev.* **38**, 460–489.

CAVAGNA, G. A., DUSMAN, B. AND MARGARIA, R. (1968). Positive work done by a previously stretched muscle. *J. appl. Physiol.* **24**, 21–32.

CHIAPPE, L. M. (1995). The first 85 million years of avian evolution. *Nature* **378**, 349–355.

COHEN, A. H., ROSSIGNOL, S. AND GRILLNER, S. (1988). *Neural Control of Rhythmic Movements in Vertebrates.* New York: John Wiley & Sons.

CUTTS, A. (1986). Sarcomere length changes in the wing muscles during the wing beat cycle of two bird species. *J. Zool., Lond.* **209**, 183–185.

DIAL, K. P. AND BIEWENER, A. A. (1993). Pectoralis muscle force and power output during different modes of flight in pigeons. *J. exp. Biol.* **176**, 31–54.

DIAL, K. P., GOSLOW, G. E., JR AND JENKINS, F. A., JR (1991). The functional anatomy of the shoulder in the European starling (*Sturnus vulgaris*). *J. Morph.* **207**, 327–344.

DIAL, K. P., KAPLAN, S. R., GOSLOW, G. E., JR AND JENKINS, F. A., JR (1988). A functional analysis of the primary upstroke and downstroke muscles in the domestic pigeon (*Columba livia*) during flight. *J. exp. Biol.* **134**, 1–16.

EDMAN, K. A. P., MULIERI, L. A. AND SCUBON-MULIEERI, B. (1976). Non-hyperbolic force–velocity relationship in single muscle fibers. *Acta physiol. scand.* **98**, 143–156.

ETTEMA, G. J. C. (1996). Elastic and length–force characteristics of the gastrocnemius of the hopping mouse (*Notomys alexis*) and the rat (*Rattus norvegicus*). *J. exp. Biol*. **199**, 1277–1285.

ETTEMA, G. J. C. AND HUIJING, P. A. (1994). Effects of distribution of muscle fiber length on active length–force characteristics of rat gastrocnemius medialis. *Anat. Rec.* **239**, 414–420.

FEDUCCIA, A. (1995). Explosive evolution in tertiary birds and mammals. *Science* **267**, 637–638.

FRIDÉN, J. AND LIEBER, R. L. (1992). Structural and mechanical basis of exercise-induced injury. *Med. Sci. Sports Exer.* **24**, 521–530.

FÜRBINGER, M. (1888). *Untersuchungen zur Morphologie und Systematik der Vögel, zugleich ein Deitrag zur Anatomie der Stütz- und Bewegungsorgane mit 30 Talfen*. Amsterdam: Holkema.

GAUNT, A. S. AND GANS, C. (1993). Variations in the distribution of motor end-plates in avian pectoralis. *J. Morph.* **215**, 65–88.

GEORGE, J. C. AND BERGER, A. J. (1966). *Avian Myology*. New York: Academic Press.

GORDON, A. M., HUXLEY, A. F. AND JULIAN, F. J. (1966*a*). Tension development in highly stretched vertebrate muscle fibres. *J. Physiol., Lond.* **184**, 143–169.

GORDON, T. R., HUXLEY, A. F. AND JULIAN, F. J. (1966*b*). The variation in isometric tension with sarcomere length in vertebrate muscle fibres. *J. Physiol., Lond.* **184**, 170–192.

GOSLOW, G. E., JR (1972). Adaptive mechanisms of the raptor pelvic limb. *Auk* **89**, 47–64.

GOSLOW, G. E., JR AND DIAL, K. P. (1990). Active stretch–shorten contractions of the M. pectoralis in the European starling (*Sturnus vulgaris*): Evidence from electromyography and contractile properties. *Neth. J. Zool.* **40**, 106–114.

GOSLOW, G. E., JR AND Van DE GRAFF, K. M. (1982). Hindlimb joint angle changes and action of the primary ankle extensor muscles durng posture and locomotion in the Striped skunk (*Mephitis mephitis*). *J. Zool., Lond.* **197**, 405–419.

HAZLEHURST, G. A. AND RAYNER, J. M. V. (1992). An unusual flight mechanism in the Pterosauria. *Palaeontology* **35**, 927–941.

JENKINS, F. A., JR (1993). The evolution of the avian shoulder joint. *Am. J. Sci.* **293** A, 253–367.

JENKINS, F. A., JR, DIAL, K. P. AND GOSLOW, G. E., JR (1988). A cineradiographic analysis of bird flight: The wishbone in starlings is a spring. *Science* **241**, 1495–1498.

JEWELL, B. R. AND WILKIE, D. R. (1958). An analysis of the mechanical components in frog's striated muscle. *J. Physiol., Lond.* **143**, 515–540.

JOYCE, G. C. AND RACK, P. M. H. (1969). Isotonic lengthening and shortening movements of cat soleus muscle. *J. Physiol., Lond.* **204**, 475–491.

JOYCE, G. C., RACK, P. M. H. AND WESTBURY, E. R. (1969). The mechanical properties of cat soleus muscle during controlled lengthening and shortening movements. *J. Physiol., Lond.* **204**, 461–474.

KARDEL, T. (1990). Niels Stensen's geometrical theory of muscle contraction (1967): A reappraisal. *J. Biomech.* **23**, 953–965.

KATZ, B. (1939). The relationship between force and speed in muscular contraction. *J. Physiol., Lond.* **96**, 45–64.

KEURS, H. E. D. J. T., IWAZUMI, T. AND POLLACK, G. H. (1978). The sarcomere length–tension relation in skeletal muscle. *J. gen. Physiol.* **72**, 565–592.

KOKSHAYSKY, N. M. (1979). Tracing the wake of a flying bird. *Nature* **279**, 146–148.

LAYLAND, J., YOUNG, I. S. AND ALTRINGHAM, J. D. (1995). The length dependence of work production in rat papillary muscles *in vitro*. *J. exp. Biol.* **198**, 2491–2499.

LIEBER, R. L. AND BROWN, C. G. (1992). Sarcomere length–joint angle relationships of seven frog hindlimb muscles. *Acta Anat.* **145**, 289–295.

LIEBER, R. L., RAAB, R., KASHIN, S. AND EDGERTON, B. R. (1992). Sarcomere length changes during swimming. *J. exp. Biol*. **169**, 251–254.

LOREN, G. J., SHOEMAKER, S. D., BURKHOLDER, T. J., JACOBSON, M. D., FRIDÉN, J. AND LIEBER, R. L. (1996). Human wrist motors: Biomechanical design and application to tendon transfers. *J. Biomech.* **29**, 331–342.

LUTZ, G. J. AND ROME, L. C. (1994). Built for jumping: The design of the frog muscular system. *Science* **263**, 370–372.

MAGID, A. AND LAW, D. J. (1985). Myofibrils bear most of the resting tension in frog skeletal muscle. *Science* **230**, 1280–1282.

MAI, M. AND LIEBER, R. L. (1990). A model of semitendinoisus muscle sarcomere length, knee and hip joint interaction in the frog hindlimb. *J. Biomech.* **23**, 271–279.

MARTIN, L. D. (1983). The origin and early radiation of birds. In *Perspctives in Ornithology* (ed. A. H. Brush and G. A. Clark, Jr), pp. 77–90. Cambridge: Cambridge University Press.

MEYERS, R. A. (1993). Gliding flight in the American kestrel (*Falco sparverius*): An electromyographic study. *J. Morph.* **215**, 213–224.

OLSON, S. L. AND FEDUCCIA, A. (1979). Flight capability and the pectoral girdle of *Archaeopteryx*. *Nature* **278**, 247–248.

OSTROM, J. H. (1969). Osteology of *Deinonychus antirrhopus*, an unusual theropod from the Lower Cretaceous of Montana. *Bull. Peabody Mus. nat. Hist.* **30**, 1–165.

OSTROM, J. H. (1976*a*). *Archaeopteryx* and the origin of birds. *Biol. J. Linn. Soc.* **8**, 91–182.

OSTROM, J. H. (1976*b*). Some hypothetical anatomical stages in the evolution of avian flight. *Smithson. cont. Paleobiol.* **27**, 1–21.

OSTROM, J. H. (1995). Wing biomechanics and the origin of bird flight. *N. Jb. Geol. Paläont. Abh.* **195**, 253–266.

OSTROM, J. H., POORE, S. O. AND GOSLOW, G. E., JR (1997). Humeral rotation and wrist supination: Important functional complex for the evolution of powered flight in birds? *Smithson. cont. Paleobiol.* **88** (in press).

PAGE, S. G. (1969). Structure and some contractile properties of fast and slow muscles of the chicken. *J. Physiol., Lond.* **205**, 131–145.

PENNYCUICK, C. J. (1986). Mechanical constraints on the evolution of flight. In *The Origin of Birds and the Evolution of Flight* (ed. K. Padian), pp. 83–98. San Francisco: California Academy of Sciences.

POORE, S. O., SANCHEZ-HAIMAN, A. AND GOSLOW, G. E., JR (1997). Wing upstroke and the evolution of flapping flight. *Nature* **387**, 799–802.

PURSLOW, P. P. AND TROTTER, J. A. (1994). The morphology and mechanical properties of endomysium in series-fibered muscles; variation with muscle length. *J. Muscle Res. Cell Motil.* **15**, 299–304.

RACK, P. M. H. AND WESTBURY, D. R. (1969). The effects of length and stimulus rate on tension in the isometric cat soleus muscle. *J. Physiol., Lond.* **204**, 443–460.

RAYNER, J. M. V. (1985). Avian flight and the problem of *Archaeopteryx*. In *Biomechanics in Evolution* (ed. J. M. U. Rayner and R. J. Wooton), pp. 183–212. Cambridge University Press.

RAYNER, J. M. V. (1988). Form and function in avian flight. *Curr. Orn.* **5**, 1–77.

RAYNER, J. M. V. (1991). Mechanical and ecological constraints on flight evolution. In *The Beginnings of Birds* (ed. M. K. Hecht, J. H. Ostrom, G. Viohl and P. Wellnhofer), pp. 279–288. Eichsätt: Jura Museum.

ROME, L. C. AND SOSNICKI, A. A. (1991). Myofilament overlap in swimming carp. II. Sarcomere length changes during swimming. *Am. J. Physiol*. **260**, C289–C296.

RUBEN, J. (1991). Reptilian physiology and the flight capacity of *Archaeopteryx*. *Evolution* **45**, 1–17.

RÜPPELL, G. (1975). *Bird Flight*. New York: Van Nostrand Reinhold Company.

SANZ, J. L., CHIAPPE, L. M., BUSCALIONI, A. D., MORATALLA, J. J., ORTEGE, F. AND POYATO-ARIZA, F. J. (1996). An Early Cretaceous bird from Spain and its implications for the evolution of avian flight. *Nature* **382**, 442–445.

SERENO, P. C. AND RAO, C. (1992). Early evolution of avian flight and perching: New evidence from the Lower Cretaceous of China. *Science* **255**, 845–848.

SIMPSON, S. F. (1983). The flight mechanism of the pigeon *Columbia livia* during take-off. *J. Zool., Lond.* **200**, 435–443.

SOKOLOFF, A., GRAY, J. AND HARRY, J. (1994). Supracoracoideus is not necesary for take-off in the starling. *Am. Zool.* **311**, 64A.

SPECTOR, S. A., GARDINER, P. F., ZERNICKE, R. Z., ROY, R. R. AND EDGERTON, V. R. (1980). Muscle architecture and force–velocity characteristics of cat soleus and medial gastrocnemius: Implications for motor control. *J. neurol. Physiol.* **44**, 951–960.

SPEDDING, G. R. (1986). The wake of a jackdaw (*Corvus monedula*) in slow flight. *J. exp. Biol.* **125**, 287–307.

SPEDDING, G. R. (1987). The wake of a kestrel (*Falco tinnunculus*) in flapping flight. *J. exp. Biol.* **127**, 59–78.

SPEDDING, G. R., RAYNER, G. M. V. AND PENNYCUICK, C. J. (1984). Momentum and energy in the wake of a pigeon (*Columba livia*) in slow flight. *J. exp. Biol.* **111**, 81–102.

STEPHENS, J. A., REINKING, R. M. AND STUART, D. G. (1975). The motor units of cat medial gastrocnemius: Electrical and mechanical properties as a function of muscle length. *J. Morph.* **146**, 495–512.

SY, M. (1936). Funktionell-anatomische Untersuchungen am Vogelflugel. *J. Ornitol.* **84**, 199–296.

TOBALSKE, B. W. AND DIAL, K. P. (1994). Neuromuscular control and kinematics of intermittent flight in budgerigars (*Melopsittacus undulatus*). *J. exp. Biol.* **187**, 1–18.

TROTTER, J. A. (1993). Functional morphology of force transmission in skeletal muscle: A brief review. *Acta Anat.* **146**, 205–222.

TROTTER, J. A. AND PUSLOW, P. P. (1992). Functional morphology of the endomysium in series fibered muscles. *J. Morph*. **212**, 109–122.

TROTTER, J., RICHMOND, F. J. R. AND PURSLOW, P. P. (1995). Functional morphology and motor control of series-fibered muscles. In *Exercise and Sports Sciences Reviews* (ed. J. Holloszy), pp. 167–213. Baltimore: American College of Sports Medicine.

TROTTER, J. A., SALGADO, J. D., OZBAYSAL, R. AND GAUNT, A. S. (1992). The composite structure of quail pectoralis muscle. *J. Morph.* **212**, 27–35.

VAZQUEZ, R. J. (1992). Functional osteology of the avian wrist and the evolution of flapping flight. *J. Morph.* **211**, 259–268.

WELLNHOFER, P. (1988). Ein neues Exempler von *Archaeopteryx*. In *Archaeopteryx.* Freunde des Jura-Museums Eichstätt. pp. 1–30.

WELLNHOFER, P. (1993). Das siebte Exemplar von *Archaeopteryx* aus den Solnhofener Schichten. In *Archaeopteryx.* Freunde des Jura-Museums Eichstätt. pp. 1–47.

YOUNG, B. A., MAGON, D. K. AND GOSLOW, G. E., JR (1990). Length–tension and histochemical properties of select shoulder muscles of the Savannah monitor lizard (*Varanus exanthematicus*): Implications for function and evolution. *J. exp. Zool.* **256**, 63–74.

ZAJAC, F. E. (1985). Thigh muscle activity during maximum-height jumps by cats. *J. Neurophysiol.* **53**, 979–994.